NEW APPROACH TO IMPACT ANALYSIS USING THE MOVING FRAME METHOD
THEORY AND NUMERICAL VALIDATION

TERJE SVÆREN

BÅRD INGE NYGÅRD

THOMAS J. IMPELLUSO

BACHELOR'S THESIS IN MECHANICAL ENIGINEERING

BERGEN, NORWAY 2019

Høgskulen på Vestlandet

NEW APPROACH TO IMPACT ANALYSIS USING THE MOVING FRAME METHOD

Terje Sværen
Bård Inge Nygård
Thomas J. Impelluso

Department of Mechanical- and Marine Engineering
Western Norway University of Applied Sciences
NO-5063 Bergen, Norway

Høgskulen på Vestlandet
Fakultet for Ingeniør- og Naturvitskap
Institutt for maskin- og marinfag
Inndalsveien 28
NO-5063 Bergen, Norge

Norsk tittel:	Ny modell for kollisjonsanalyse ved bruk av ''The Moving Frame Method''

Author(s), student number:	Terje Sværen, h148015
	Bård Inge Nygård, h181334
	Thomas J. Impelluso

Study program:	Mechanical Engineering
Date:	June 2019
Report number:	IMM 2019-M19
Supervisor at HHVL:	Thomas J. Impelluso
Assigned by:	ABB
Contact person:	Kristian Johannessen

Antall filer levert digitalt:	1

DRAFT IMECE2019-XXXXX

NEW APPROACH TO IMPACT ANALYSIS USING THE MOVING FRAME METHOD: THEORY AND NUMERICAL VALIDATION

Terje Sværen
Marine Engineering
Western Norway University of
Applied Sciences
(HVL), Bergen, Norway
terjesvaeren@hotmail.com

Bård Inge Nygård
Marine Engineering
Western Norway University of
Applied Sciences
(HVL), Bergen, Norway
bin.1994@hotmail.com

Thomas J. Impelluso
Marine Engineering
Western Norway University of
Applied Sciences
(HVL), Bergen, Norway
tjm@hvl.no

ABSTRACT

This research puts forth a framework with which others can deliver future collision models. While this delivers the framework through the coefficient of restitution, others may use different constitutive approaches. The coefficient of restitution is a phenomenological constant that enables engineers to model and classify collisions. This work retains the simplicity of that phenomenological constant, to create a spatial collision framework for rapid deployment, while delivering a methodology that has the potential for more advanced modeling by others. In this research, we use the Moving Frame Method (MFM) in dynamics, to calculate the contact forces, impact, trajectory/translation and rotation after impact of free bodies in 3D space. The MFM exploits Cartan's notion of moving frames to place frames of reference on all moving bodies. In this way, we formulate the dynamics in each body's own moving frame. Next, the MFM exploits Lie group theory SO(3) and its associated algebra, so(3), to relate such frames to each other. Finally, it exploits a new notation to simplify the mathematics. All of this expedites the extraction of the post-collision dynamics. We also conduct a numerical validation of the results, as follows. We simulate a collision using MSC Adams and compare the rotation and translation values of the bodies with what we found using MFM. After presenting the simpler aspects of the theory for edification's sake, we pinpoint the aspects that can encompass alternative models. Finally, we display results on a 3D web page using WebGL

NOMENCLATURE

α : General body number
$\mathbf{e}^{(\alpha)}$: Moving Frame
$\mathbf{e}^I$: Inertial Frame
$\mathbf{r}$: Absolute Position Vector
$\mathbf{s}$: Relative Position Vector

e : Coefficient of Restitution (COR)
R : Rotation Matrix
$\boldsymbol{\omega}$: Angular Velocity Vector
ω : Components of angular velocity
$\overset{\leftrightarrow}{\omega}$: Skew Symmetric Angular Velocity Matrix
$\mathbf{H}_C$: Angular Momentum Vector
$\mathbf{L}$: Linear Momentum Vector
$J_C^{(\alpha)}$: 3x3 Mass Moment of Inertia Matrix
I_{3x3} : 3x3 Identity matrix
$\mathbf{F}$: Force vector
$\mathbf{M}_C = \dot{\mathbf{H}}_C$: Moment vector

INTRODUCTION

Engineers define impact as the collision between two bodies during a finitely small increment of time.

The laws of linear and angular momentum are accurate, true and fundamental for the analysis of classical engineering collision problems. If one studies the collision of rigid bodies, one may conduct the analysis under the mathematical framework of rigid body dynamics. However, if one allows for the deformation of object, the analysis opens up too many approaches. We will touch on just a few, as we do not intend this as a definitive survey.

Some approaches to collision analysis, such as Wu [1], take recourse to finite element methods to assess material deformation during the collision.

Gildardi and Sharf [2] suggest that the goal of collision studies is to obtain a simple model based on known parameters prior to the impact; e.g., the coefficient of restitution.

Collision analyses are difficult because of their complexity. One must account for the geometry and material properties of both bodies. One also must account for the smoothness of the colliding surfaces or friction Wang [3]. In many cases, the speed of the collision also plays a role, as per Minamoto [4], or Gharib [5].

In general, the result of a collision could be determined if all mechanical interactions (including, say, nonlinear constitutive laws for each body) could be captured and inserted into the mathematical model.

Other studies model additional relationships between collision forces and local deformation under various loading conditions, such as that done by Hunt [6]. All of these models attempt to infuse the fundamental assumptions regarding contact forces. Ahmad [7] has conducted a comprehensive survey of existing collision models. We hope to add to this discussion with a framework for future models.

Once one obtains a coefficient of restitution, engineers proceed with a wide array of analyses in diverse disciplines. Cross [8] conducted work in sports dynamics, Batista [9] in Automotive Dynamics and Vasilopoulos [10] in robotics.

In this effort, we endeavor to develop, less a model, but more so, a framework for future models. To deliver this framework, we leverage the simplicity of the coefficient of restitution. We aspire to deliver a framework that one can rapidly deploy for an array of constitutive models, for many applications.

A current application of collision studies is by ABB, Inc. ABB has been developing subsea electrical equipment that can reliably provide power to depths down to 3,000 meters. The equipment must operate at immense pressures in a highly corrosive environment with little or no maintenance. More important, the engineers must find safe ways to deposit the equipment on the seabed. Thus, ABB must consider, in their design analyses of the lowered structure, the interaction/collision of the object with the mounting structure. Depending on parameters such as speed, material, damping, stiffness, contact area, etc., ABB is interested in understanding the magnitude of the collision forces on the outer enclosures of the subsea equipment and the effect of these forces on the integrity of the enclosed electrical/electronic equipment.

It is both the theoretical advance of the MFM and the needs of ABB that motivate the project introduced in this paper—to improve collision models.

The coefficient of restitution is at the core of our current framework (others can be used), and warrants brief mention. A kinematic analysis presumes the coefficient depends on velocities. A kinetic analysis presumes the coefficient depends on contact forces. An energy analysis presumes the coefficient depends on the work done during the impact. All of these can enable the analysis, by setting up a phenomenological constant: the coefficient of restitution. Many studies restrict themselves to obtaining the coefficient of restitution through experimental analyses.

This research hopes to add to achievements in collision modeling, with a modernized mathematical framework for spatial body motion after collision. For this, we turn to the Moving Frame Method and develop the necessary equations so that others will have access to a new framework based on modern mathematics.

MOVING FRAME METHOD

Background
Galileo Galilei (1564-1642) imagined, through thought experiments, that people inside a closed, covered, ship are unable to determine by measurements made inside the ship, whether they were moving. We cannot sense velocity but we can sense acceleration.

Isaac Newton (1643-1727) based his laws of motion on acceleration. He equipped the discipline with vector calculus: the mathematics of change (of magnitude and direction). He embraced the primacy of inertial frames from which one could study a particle's motion. He focused attention on particles, not bodies.

Leonard Euler (1707-1783) extended Newton's laws for particles to model the rotations of bodies. However, he, too, relied on vector algebra.

By this time, the Industrial Revolution dawned (1800-1950). The steam engine, locomotives, lathes, sewing machines, and other mechanical mechanisms were simple one- or two-dimensional devices, rotating in a plane and viewed from the perspective of an inertial user standing beside them.

These engineering achievements, mathematical principles and observations "informed" the dynamics curriculum. The current undergraduate curriculum, for example, in dynamics privileges the inertial frame, focuses on planar rotations, and limits itself with vector algebra. These restrictions are fraught with obfuscations that confound those students who do not possess the internal visualization skills needed to overcome the limits of an outmoded mathematics.

As the undergraduate dynamics curriculum focused on two-dimensional (2D) problems, mathematicians were progressing in more exciting directions.

Élie Cartan (1869-1951) [12] assigned a reference frame to each point of an object under study (a curve, a surface, Euclidean space itself). Then, using an orthonormal expansion, he expressed the rate of change of the frame in terms of the frame. The MFM leverages this by placing a reference frame on every

moving link. However, then we need to connect moving frames. For this, we turn to Sophus Lie.

Marius Sophus Lie (1842-1899) developed the theory of continuous groups and their associated algebras. The MFM adopts the mathematics of rotation groups and their algebras yet distils them to simple matrix multiplications that avoids the non-associative properties of vectors. However, then we need a simplifying notation. For this, we turn to Frankel.

Ted Frankel [12] developed a compact notation in his work on geometrical physics. The MFM adopts this notation to enable a methodology that is identical for both 2D and 3D analyses. The notation is also identical for single bodies and multi-body linked systems.

Before we present the theory of 3D collisions, we first summarize the most basic foundation of the MFM.

The MFM: Kinematics

The middle image in Figure 1 presents, in light grey, an inertial orthogonal Cartesian coordinate system, designated by $\{x_1, x_2, x_3\}$, where the subscripts designated one of three directions.
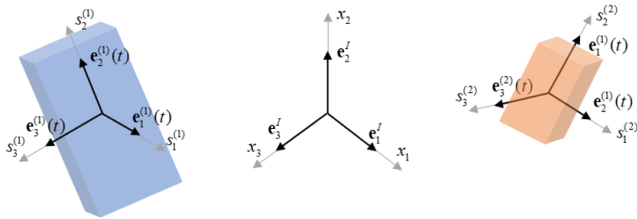

FIGURE 1. FRAME RELATIONS

Frame basis vectors derive from directional derivatives of coordinate functions: $\mathbf{e}_i^I \equiv \partial / \partial x_i$.

Thus, the middle image of Figure 1 also presents the associated inertial frame basis vectors designated by $\mathbf{e}^I = \begin{pmatrix} \mathbf{e}_1^I & \mathbf{e}_2^I & \mathbf{e}_3^I \end{pmatrix}$ in bold black, with superscript "I".

The left image of Fig. 1 presents a blue moving body. A moving coordinate system designated by $\{s_1^{(1)}, s_2^{(1)}, s_3^{(1)}\}$ is embedded on the moving body—superscript (1). The same left side also presents the associated time dependent moving frame: $\mathbf{e}^{(1)}(t) = \begin{pmatrix} \mathbf{e}_1^{(1)}(t) & \mathbf{e}_2^{(1)}(t) & \mathbf{e}_3^{(1)}(t) \end{pmatrix}$.

The right side of Fig. 1 presents similar information for a second moving body. Let us now focus on the orientation of the frames.

We designate $R^{(1)}(t)$ as a 3×3 orthogonal rotation matrix. This rotation matrix describes the orientation of the moving body

frame $\mathbf{e}^{(1)}(t)$ (a row vector) from the inertial frame $\mathbf{e}^I$ (also a row vector) through post-multiplication (where dimensions are presented below each term):

$$\begin{pmatrix} \mathbf{e}_1^{(1)}(t) & \mathbf{e}_2^{(1)}(t) & \mathbf{e}_3^{(1)}(t) \end{pmatrix} = \underset{1\times3}{\begin{pmatrix} \mathbf{e}_1^I & \mathbf{e}_2^I & \mathbf{e}_3^I \end{pmatrix}} \underset{3\times3}{R(t)} \qquad (1)$$

Orthogonality of rotation matrices, as members of the SO(3) group, allows an analytical inverse as the transpose:

$$\mathbf{e}^{(1)}(t)R(t)^T = \mathbf{e}^I \qquad (2)$$

The rate of change of the frame, supplemented with the orthogonality, allows the following progression, reading left to right, with the following definition $\overrightarrow{\omega^{(1)}(t)} \equiv R(t)^T \dot{R}(t)$:

$$\dot{\mathbf{e}}^{(1)}(t) = \mathbf{e}^I \dot{R}(t) = \mathbf{e}^{(1)}(t)R(t)^T \dot{R}(t) \equiv \mathbf{e}^{(1)}(t)\overrightarrow{\omega^{(1)}(t)}$$

$$= \mathbf{e}^{(1)}(t) \begin{bmatrix} 0 & -\omega_3^{(1)}(t) & \omega_2^{(1)}(t) \\ \omega_3^{(1)}(t) & 0 & -\omega_1^{(1)}(t) \\ -\omega_2^{(1)}(t) & \omega_1^{(1)}(t) & 0 \end{bmatrix} \qquad (3a)$$

Here we defined $\overrightarrow{\omega^{(1)}(t)} \equiv R(t)^T \dot{R}(t)$ as angular velocity matrix (as distinct from the angular velocity vector). Its properties, such as skew symmetry, derive from the group's associated algebra so(3). One can isomorphically reconstruct the angular velocity vector, in which the coordinates and the frame basis are functions of time.

$$\boldsymbol{\omega}^{(1)}(t) = \mathbf{e}^{(1)}(t) \begin{pmatrix} \omega_1^{(1)}(t) \\ \omega_2^{(1)}(t) \\ \omega_3^{(1)}(t) \end{pmatrix} \qquad (3b)$$

In Equation (3a) we find a statement of the angular velocity, in which even the frame may change direction, with time.

For completeness, we assert that $\mathbf{s}_P = \mathbf{e}(t)s_P(t)$ locates points, (which may in turn, be moving) in a moving body frame. We then take time derivatives as follows.

$$\mathbf{v}_P(t) = \dot{\mathbf{s}}_P(t) = \dot{\mathbf{e}}(t)s_P(t) + \mathbf{e}(t)\dot{s}_P(t)$$
$$\mathbf{v}_P(t) = \mathbf{e}(t)\overrightarrow{\omega(t)}s_P(t) + \mathbf{e}(t)\dot{s}_P(t) = \mathbf{e}(t)\left(\overrightarrow{\omega(t)}s_P(t) + \dot{s}_P(t)\right)$$

$$\mathbf{a}_P(t) = \ddot{\mathbf{s}}_P(t) = \dot{\mathbf{e}}(t)\left(\overrightarrow{\omega(t)}s_P(t) + \dot{s}_P(t)\right) + \mathbf{e}(t)\left(\overrightarrow{\dot{\omega}(t)}s_P(t) + \ddot{s}_P(t)\right)$$
$$\mathbf{a}_P(t) = \ddot{\mathbf{s}}_P(t) = \mathbf{e}(t)\left(\ddot{s}_P(t) + \overrightarrow{\omega(t)}\overrightarrow{\omega(t)}s_P(t) + 2\overrightarrow{\omega(t)}\dot{s}_P(t) + \overrightarrow{\dot{\omega}(t)}s_P(t)\right)$$

This last equation identifies, left to right, the linear, centripetal, Coriolis and angular accelerations in one equation, 2D and 3D, using matrix notation, and no cross products, with the one frame clearly stated.

The MFM: Kinetics

We continue our summary, turning now to kinetics. The reader may find a pedagogical based description in Impelluso [13]. The MFM formulates Newton's and Euler's Equations for frames at the center of mass of a body (free bodies) and for frames at joints (robotics). This section will only summarize the formulation of these kinetic laws of motion, but only for frames at the center of mass and only for non-jointed bodies.

We begin by integrating over all the mass elements to structure the form of the linear and angular momentum. This represents the first two lines in Table 1.

TABLE 1
Summary of Newton and Euler Equations in moving body frame

	LINEAR	ANGULAR
Definition of momentum: Integral form	$\mathbf{L}(t)=\int_B \mathbf{v}_P \, d\,m_P$	$\mathbf{H}_C(t) \equiv \int_{B(t)} \mathbf{s}_P \times \dot{\mathbf{s}}_P dm_P$
Derived Coordinate definition	$\mathbf{L}(t)=\mathbf{e}(t)\,m v_C(t)$	$\mathbf{H}_C(t)=\mathbf{e}(t)\,J_C\,\omega(t)$
Derivative of coordinate definition	$\dot{\mathbf{L}}(t)=\mathbf{e}(t)\,m\dot{v}_C(t)+ \dot{\mathbf{e}}(t)\,m v_C(t)$	$\dot{\mathbf{H}}_C(t)=\mathbf{e}(t)\,J_C\,\dot{\omega}(t)+ \dot{\mathbf{e}}(t)\,J_C\,\omega(t)$
Exploiting angular velocity matrix	$\dot{\mathbf{L}}(t)=\mathbf{e}(t)\, m\left(\dot{v}_C(t)+\overrightarrow{\omega(t)}\,v_C(t)\right)$	$\dot{\mathbf{H}}_C(t)=\mathbf{e}(t)\, \left(J_C\dot{\omega}(t)+\overrightarrow{\omega(t)}J_C\,\omega(t)\right)$
Kinetic expression	$\dot{\mathbf{L}}(t)=\mathbf{F}(t)$	$\dot{\mathbf{H}}_C(t)=\mathbf{M}_C(t)$
Component form	$F(t)=m\left(\dot{v}_C(t)+\overrightarrow{\omega(t)}\,v_C(t)\right)$	$M_C(t)=J_C\,\dot{\omega}(t)+ \overrightarrow{\omega(t)}J_C\,\omega(t)$

In the second row of the first column, we find a vector based assertion of linear momentum. In the second row of the second column, we find a coordinate based assertion of the angular momentum, also stated in a moving, yet explicitly stated, body frame.

In the equations in this table, the column components of the angular velocity derive from the skew symmetric angular velocity matrix for the moving body. Furthermore, J_C represents the body's moment of inertia matrix.

Next, we take derivatives (again, this is merely a summary). The final row of each column presents the coordinate expressions for Newton's and Euler's laws. We will discuss additional aspects of the MFM as we apply it to collision studies.

MFM APPLIED TO CONTACT

We now use the MFM to structure collision behavior. We choose to base this on the coefficient of restitution; however, others may use this framework to base it on other constitutive models.

It may initially appear that a great deal of the following work is regurgitation from the college pedagogy of particle collisions. We ask the indulgence of the reader, for the power of the MFM becomes evident, later into this discussion.

Consider the incipient collision of the two bodies in Figure 1, but detailed in Figure 2 (which evinces the eccentric nature of the collision). Assume the time definitions in Table 2, and that there comes an instant, as the bodies collide, when the internal force of impact, peaks.
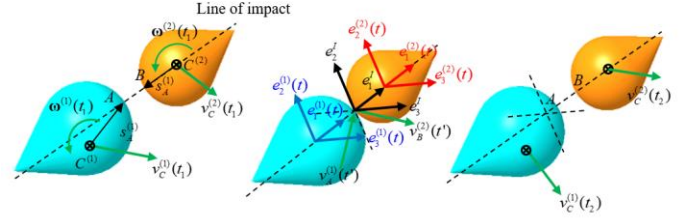
FIGURE 2. COLLIDING BODIES

As with the standard approach to all contact problems, we assert the time interval, while not infinitesimally small, is sufficiently small for the stated assumptions of this analysis, below.

TABLE 2
Time of Contact

Symbol	Description
t_1	Loading is incipient; the bodies are poised to contact (separated here, only for image clarity)
t'	Peak loading: loading has completed, and unloading commences
t_2	Unloading has completed; the bodies are poised to separate.

For this introductory study, we assume, for ease, a convex outer surface to limit the possibility of bodies to re-collide.

Assert the following definitions, notations and additional assumptions:

- Point $C^{(1)}$ represents the center of mass of body 1.
- Point $C^{(2)}$ represents the center of mass of body 1.
- Point A represents the point on body-1 that makes contact with body-2.
- Point B represents the point on body-2 that makes contact with body-1.
- This common point is the *contact point:* $A \equiv B : @ t = t'$.
- A plane through $A \equiv B : @ t = t'$, tangent to the external surfaces is the *plane of contact.*
- The *line of contact* passes through $A \equiv B : @ t = t'$ and is perpendicular to the *plane of contact.*

- Assume the *contacting bodies are frictionless at the contact surface.*
- Assume the contact forces are parallel to the line of impact (frictionless contact).
- The green vectors represent the current translational velocity of the CM

We categorize two possible types of collisions:

- If the centers of mass of each body are on the line of impact, we classify the impact as *central impact.*
- If either of the two centers of mass are not on the extended line of impact, we classify the impact as *eccentric impact.*

At $t = t'$, when point A and B are spatially coincident, establish the origin of an inertial frame, $\mathbf{e}^I \equiv \begin{bmatrix} \mathbf{e}_1^I & \mathbf{e}_2^I & \mathbf{e}_3^I \end{bmatrix}$, as shown in Figure 1, as follows:

- The first axis, $\mathbf{e}_1^I$, is directed along the *line of impact* and points from body-1 to body-2.
- The second, tangent, axis $\mathbf{e}_2^I$ is orthogonal in space, to $\mathbf{e}_2^I$
- The third, tangent, axis $\mathbf{e}_3^I$ can be constructed from the right hand rule.

Before we turn to kinetics in moving frames, we say a few words about the deposition of frames. In the application of the MFM, we would normally attach a body frame to each moving body—for the power of the MFM is that it formulates all of dynamics in moving frames. Furthermore, moving frames lend clarity to the various non-inertial forces such as Coriolis and Centrifugal (see Impelluso [13]).

If needed, we deposit an inertial frame from a moving frame using the pointwise principle of Euclidean space. However, we avoid that approach in this analysis. In this analysis, we will place the inertial frame at what is predetermined to be the contact point through some search algorithm that checks for incipient collision. Any such algorithm should be able to define the direction of collision and the contact points on each body; but this is not our concern.

Newton's Laws for the Case of Spatial Eccentric Impact between Two Free Bodies

We state Newton's Law for each body (the rate of change of linear momentum is equal to the applied forces):

$$\dot{\mathbf{L}}^{(1)}(t) = \mathbf{F}^{(1)}(t) \qquad \dot{\mathbf{L}}^{(2)}(t) = \mathbf{F}^{(2)}(t) \qquad (4a,b)$$

Let us now distinguish the overall contact forces by their two distinct phases (where we place a hat on the unloading force to emphasize, notationally, its distinction from the representation of rotation matrices):

- A time-dependent *normal* contact force during loading: $\mathbf{P}(t)$ for $t_1 < t < t'$
- A time-dependent *normal* contact force during unloading: $\hat{\mathbf{R}}(t)$ for $t' < t < t_2$

We may now represent the force on each body in the inertial frame, at the instant of contact. Assume the positive direction of this contact force lies in the $\mathbf{e}_1^I$ direction.

The following holds for the duration of the loading phase $t_1 < t < t'$, recollecting that we are assuming frictionless contact (thus only one component).

$$\mathbf{P}^{(1)}(t) = -\mathbf{e}^I \begin{pmatrix} P_1(t) \\ 0 \\ 0 \end{pmatrix} \qquad \mathbf{P}^{(2)}(t) = \mathbf{e}^I \begin{pmatrix} P_1(t) \\ 0 \\ 0 \end{pmatrix} \qquad (5a,b)$$

The following holds for the duration of the unloading phase $t' < t < t_2$, recollecting that we are assuming frictionless contact (thus only one component).

$$\hat{\mathbf{R}}^{(1)}(t) = -\mathbf{e}^I \begin{pmatrix} \hat{R}_1(t) \\ 0 \\ 0 \end{pmatrix} \qquad \hat{\mathbf{R}}^{(1)}(t) = \mathbf{e}^I \begin{pmatrix} \hat{R}_1(t) \\ 0 \\ 0 \end{pmatrix} \qquad (6a,b)$$

Next, state the Linear Momentum for the center of mass, C, for each body, but in that body's moving frame:

$$\mathbf{L}^{(1)}(t) = \mathbf{e}^{(1)}(t) m^{(1)} v_C^{(1)}(t)$$
$$\mathbf{L}^{(2)}(t) = \mathbf{e}^{(2)}(t) m^{(2)} v_C^{(2)}(t) \qquad (7a,b)$$

As per Table 1, assert the rate of change of the linear momentum.

$$\dot{\mathbf{L}}^{(1)}(t) = \mathbf{e}^{(1)} m^{(1)} \left(\dot{v}_C^{(1)}(t) + \overrightarrow{\omega^{(1)}(t)} \, v_C^{(1)}(t) \right)$$
$$\dot{\mathbf{L}}^{(2)}(t) = \mathbf{e}^{(2)} m^{(2)} \left(\dot{v}_C^{(2)}(t) + \overrightarrow{\omega^{(2)}(t)} \, v_C^{(2)}(t) \right) \qquad (8a,b)$$

To proceed, we must extract components. To extract the components, we must select one common frame. We choose to do this work in the moving frame; thus, we must reassert the forces in the moving frame, through some rotation matrix (one superscript for each body) using Eqn. 2. Finally, we equate the rate of change of linear momentum with force, extract the components and obtain:

TABLE 3
Newton's Equation for each body for both loading and unloading

Loading		
Body 1	*Body 2*	
$m^{(1)}\left(v_{C1}^{(1)}(t') - v_{C1}^{(1)}(t_1)\right) = -\int_{t_1}^{t'} P(t)dt$	$m^{(2)}\left(v_{C1}^{(2)}(t') - v_{C1}^{(2)}(t_1)\right) = \int_{t_1}^{t'} P(t)dt$	(9a,b)
Unloading		
Body 1	*Body 2*	
$m^{(1)}\left(v_{C1}^{(1)}(t_2) - v_{C1}^{(1)}(t')\right) = -\int_{t'}^{t_2} \hat{R}(t)dt$	$m^{(2)}\left(v_{C1}^{(2)}(t_2) - v_{C1}^{(2)}(t')\right) = \int_{t'}^{t_2} \hat{R}(t)dt$	(10a,b)

For the sake of edification, it is wise to apply some restrictions, early on. We will decide, in this problem, that the body frame of the first and second body remain parallel to the inertial frame, during the duration of loading and unloading. Thus, in this pedagogical presentation, the rotation matrices are the identity matrices. We will relieve ourselves of this restriction in the summary when we suggest how others may expand this work.

Most important, keep in mind the distinction between points that make contact—A on body 1, B on body 2—versus the center of mass, C1, on body 1 and C2 on body 2. Until we state otherwise, the following discussion concerns Newton's laws asserted at the center of mass, Ci, of each body, not contact points.

We integrate just the first components from each of the previous equations. We do this between the temporal boundaries of the loading and unloading phases. We express the normal components without subscript as: $P(t) = P_1(t)$ and $\hat{R}(t) = \hat{R}_1(t)$

TABLE 4
Integration of Components of Newton's Equation for each body for both phases

Loading		
Body 1	*Body 2*	
$m^{(1)}\left(v_{C1}^{(1)}(t') - v_{C1}^{(1)}(t_1)\right) = -\int_{t_1}^{t'} P(t)dt$	$m^{(2)}\left(v_{C1}^{(2)}(t') - v_{C1}^{(2)}(t_1)\right) = \int_{t_1}^{t'} P(t)dt$	(11a,b)
Unloading		
Body 1	*Body 2*	
$m^{(1)}\left(v_{C1}^{(1)}(t_2) - v_{C1}^{(1)}(t')\right) = -\int_{t'}^{t_2} \hat{R}(t)dt$	$m^{(2)}\left(v_{C1}^{(2)}(t_2) - v_{C1}^{(2)}(t')\right) = \int_{t'}^{t_2} \hat{R}(t)dt$	(12a,b)

We now add all four of Equations (11) and (12), canceling the total impulse terms and the velocities at peak impact. (The other two directions have no change in the velocity due to the no-friction assumption.) We have re-derived the conservation of linear momentum:

$$m^{(1)}v_{C1}^{(1)}(t_1) + m^{(2)}v_{C1}^{(2)}(t_1) = m^{(1)}v_{C1}^{(1)}(t_2) + m^{(2)}v_{C1}^{(2)}(t_2) \quad (13)$$

We assume we know the incipient velocities on the left side of (13); we assume the right side is unknown. This (and the following few comments) continue to remain identical to the traditional approaches; the power of the MFM is pending.

Assert the following as the *total* loading and unloading forces in the contact direction:

- The *total impulse* of the impending contact force during the loading phase: $\int_{t_1}^{t'} Pdt$.

- The *total impulse* of the restitution contact force during the unloading phase: $\int_{t'}^{t_2} Rdt$.

Define the *coefficient of restitution* as the ratio of these total impulse values:

$$e \equiv \int_{t'}^{t_2} R(t)dt \, / \int_{t_1}^{t'} P(t)dt \quad (14)$$

We will treat this value as a phenomenological constant, in our analysis. Others may choose alternate paths.

We apply the definition of the coefficient of restitution (14) to (12a):

$$m^{(1)}\left(v_{C1}^{(1)}(t_2) - v_{C1}^{(1)}(t')\right) = -\int_{t'}^{t_2} \hat{R}(t)dt = -e\int_{t_1}^{t'} P(t)d\tau \quad (15)$$

Combining (15) with (11a), we find:

$$v_{C1}^{(1)}(t_2) - v_{C1}^{(1)}(t') = e\left(v_{C1}^{(1)}(t') - v_{C1}^{(1)}(t_1)\right) \quad (16)$$

We repeat this for body-2 and we obtain the equation:

$$v_{C1}^{(2)}(t_2) - v_{C1}^{(2)}(t') = e\left(v_{C1}^{(2)}(t') - v_{C1}^{(2)}(t_1)\right) \quad (17)$$

We remind ourselves that these two equations apply only for the 1-direction.

At this point, we should progress to the assumption that at the time, t', of extreme impact, the velocities of the contact material points on the colliding bodies will be the same. To assert this, we need to assert the velocities of the *material* points (A, and B) from the velocities of the respective centers of mass. For this, we will exploit the paraphernalia of moving frames. This will necessarily demand we pay attention to body rotations. Thus, we decide to discuss these body rotations *first*, in the context of Euler's equations, before we apply our constraint on the contacting point's velocities (just to gain more familiarity with the MFM).

Euler's Laws for the Case of Spatial Eccentric Impact between Two Free Bodies

We now apply Euler's equation about each body's center of mass:

$$\dot{\mathbf{H}}_C^{(1)}(t) = \mathbf{M}_C^{(1)}(t) \qquad \dot{\mathbf{H}}_C^{(2)}(t) = \mathbf{M}_C^{(2)}(t) \qquad (18a,b)$$

A Notational Digression

Before we continue, allow us to re-inform the cross product. Given two vectors, each in their own frame, we assert, using Frankel's compact notation as follows:

$$\mathbf{v} = \begin{pmatrix} \mathbf{e}_1(t) & \mathbf{e}_1(t) & \mathbf{e}_1(t) \end{pmatrix} \begin{pmatrix} v_1(t) \\ v_2(t) \\ v_3(t) \end{pmatrix} \qquad \mathbf{w} = \begin{pmatrix} \mathbf{e}_1(t) & \mathbf{e}_1(t) & \mathbf{e}_1(t) \end{pmatrix} \begin{pmatrix} w_1(t) \\ w_2(t) \\ w_3(t) \end{pmatrix}$$

$$\mathbf{v} \times \mathbf{w} = \begin{pmatrix} \mathbf{e}_1(t) & \mathbf{e}_1(t) & \mathbf{e}_1(t) \end{pmatrix} \begin{bmatrix} 0 & -v_3(t) & v_2(t) \\ v_3(t) & 0 & -v_1(t) \\ -v_2(t) & v_1(t) & 0 \end{bmatrix} \begin{pmatrix} w_1(t) \\ w_2(t) \\ w_3(t) \end{pmatrix} = \mathbf{e}(t) \overrightarrow{v(t)} w(t)$$

Moments

Continuing, since the collision is eccentric, let us introduce new geometric terms: the moment arms from each body's center of mass, to the appropriate contact points—$\mathbf{s}_A^{(1)}(t)$, $\mathbf{s}_B^{(2)}(t)$—stated in the inertial frame. We take the coordinates of these points and assert them as skew symmetric form in preparation for their use in the cross product operation.

$$\overrightarrow{s_A^{(1)}(t)} = \begin{bmatrix} 0 & -s_{A3} & s_{A2} \\ s_{A3} & 0 & -s_{A1} \\ -s_{A2} & s_{A1} & 0 \end{bmatrix} \qquad \overrightarrow{s_B^{(2)}(t)} = \begin{bmatrix} 0 & -s_{B3} & s_{B2} \\ s_{B3} & 0 & -s_{B1} \\ -s_{B2} & s_{B1} & 0 \end{bmatrix}$$
$$(19a,b)$$

We now assert components of the loading equations (18a, b) as follows (where the un-subscripted omega represents all three angular velocity components in the moving body frame):

$$\mathbf{M}_{C-Loading}^{(1)}(t) = -\mathbf{e}^I \overrightarrow{s_A^{(1)}(t)} P(t) = -\mathbf{e}^{(1)} R^{(1)}(t)^T \overrightarrow{s_A^{(1)}(t)} P(t)$$
$$\mathbf{M}_{C-Loading}^{(2)}(t) = \mathbf{e}^I \overrightarrow{s_B^{(2)}(t)} P(t) = \mathbf{e}^{(2)} R^{(2)}(t)^T \overrightarrow{s_B^{(2)}(t)} P(t) \qquad (20a,b)$$

In (20), the terms in the middle represent the moment in the inertial frame. In the far right, we assert the moment in the moving body frame using the orthogonality of the rotation matrix.

We now repeat this work for the unloading period:

$$\mathbf{M}_{C-unloading}^{(1)}(t) = -\mathbf{e}^I \overrightarrow{s_A^{(1)}(t)} \hat{R}(t) = -\mathbf{e}^{(1)} R^{(1)}(t) \overrightarrow{s_A^{(1)}(t)} \hat{R}(t)$$
$$\mathbf{M}_{C-unloading}^{(2)}(t) = \mathbf{e}^I \overrightarrow{s_B^{(2)}(t)} \hat{R}(t) = \mathbf{e}^{(2)} R^{(2)}(t) \overrightarrow{s_B^{(2)}(t)} \hat{R}(t) \qquad (21a,b)$$

We must reconcile the two different frames in Equation (20) and (21). We asserted that we deposited the inertial frame at the time of peak contact. Furthermore, for each body, we oriented the two body frames at that same time. Thus, we recognize: $R^{(1)}(t') = I = R^{(2)}(t')$.

Naturally, the reader is free to amend this for more advanced collision models.

Finally, we remove the time dependency from the moment arm, by assuming any deformation is negligible (however, the reader is free to amend this, too).

As an aside, we assumed aligned axes to produce a diagonal moment of inertia matrix, for the sake of edification. We will also relieve this restriction, in the summary. Thus, we obtain the following:

TABLE 5
Moments on each body for Loading and Unloading

Loading		
Body 1	*Body 2*	
$\mathbf{M}_{C-Loading}^{(1)}(t) = \mathbf{e}^{(1)}(t) \begin{pmatrix} 0 \\ -s_{A3}P_1(t) \\ s_{A2}P_1(t) \end{pmatrix}$	$\mathbf{M}_{C-Loading}^{(2)}(t) = \mathbf{e}^{(2)}(t) \begin{pmatrix} 0 \\ s_{B3}P_1(t) \\ -s_{B2}P_1(t) \end{pmatrix}$	(22a,b)
Unloading		
Body 1	*Body 2*	
$\mathbf{M}_{C-Unloading}^{(1)}(t) = \mathbf{e}^{(1)}(t) \begin{pmatrix} 0 \\ -s_{A3}\hat{R}_1(t) \\ s_{A2}\hat{R}_1(t) \end{pmatrix}$	$\mathbf{M}_{C-Unloading}^{(2)}(t) = \mathbf{e}^{(2)}(t) \begin{pmatrix} 0 \\ s_{B3}\hat{R}_1 \\ -s_{B2}\hat{R}_1 \end{pmatrix}$	(23a,b)

Rate of change of Angular Momentum

For any time, we have the general form (where, for space limits, we focus on body 1):

$$\dot{\mathbf{H}}_C^{(1)}(t) = \mathbf{e}^{(1)} \overrightarrow{\omega^{(1)}(t)} J \omega^{(1)}(t) + J \dot{\omega}^{(1)}(t) \qquad (24)$$

$$\dot{\mathbf{H}}_C^{(1)}(t) = \mathbf{e}^{(1)} \left(\begin{pmatrix} -J_2^{(1)} \omega_2^{(1)}(t)\omega_3^{(1)}(t) + J_3^{(1)} \omega_2^{(1)}(t)\omega_3^{(1)}(t) \\ J_1^{(1)} \omega_1^{(1)}(t)\omega_3^{(1)}(t) - J_3^{(1)} \omega_1^{(1)}(t)\omega_3^{(1)}(t) \\ -J_1^{(1)} \omega_1^{(1)}(t)\omega_2^{(1)}(t) + J_2^{(1)} \omega_2^{(1)}(t)\omega_1^{(1)}(t) \end{pmatrix} + \begin{pmatrix} J_1^{(1)} \dot{\omega}_1^{(1)}(t) \\ J_2^{(1)} \dot{\omega}_2^{(1)}(t) \\ J_3^{(1)} \dot{\omega}_3^{(1)}(t) \end{pmatrix} \right) \qquad (25)$$

At this point, we continue with some assumptions. We assume there is no angular velocity about the line of contact, and the angular acceleration about that line is negligible: $\dot{\omega}_1^{(1)}(t) = \omega_1^{(1)}(t) = 0$.

Thus, we find, for the rate of change of angular momentum, in general:

$$\dot{\mathbf{H}}_C^{(1)}(t) = \mathbf{e}^{(1)} \begin{Bmatrix} -J_2^{(1)}\omega_2^{(1)}(t)\omega_3^{(1)}(t) + J_3^{(1)}\omega_2^{(1)}(t)\omega_3^{(1)}(t) \\ J_2^{(1)}\dot{\omega}_2^{(1)}(t) \\ J_3^{(1)}\dot{\omega}_3^{(1)}(t) \end{Bmatrix} \quad (26)$$

We discard the first equation in each set (for the 1-coordinate), as it concerns change in rotation about the 1-axis (the impact force is in the 1-direction, and this nulls out the resulting moments). We now formulate Euler's equation, after also assuming rigid bodies (and removing the time dependency from the moment arm).

Finally, assuming rigid body contact, remove the time dependency from the moment arms.

TABLE 6
Euler's equation for each body during both phases

	Loading	Unloading
Body 1; *Rotation about 2*	$J_2^{(1)}\dot{\omega}_2^{(1)}(t) = -s_{A3}P(t)$	$J_2^{(1)}\dot{\omega}_2^{(1)}(t) = -s_{A3}\hat{R}(t)$
Body 1; *Rotation about 3*	$J_3^{(1)}\dot{\omega}_3^{(1)}(t) = s_{A2}P(t)$	$J_3^{(1)}\dot{\omega}_3^{(1)}(t) = s_{A2}\hat{R}(t)$
Body 2; *Rotation about 2*	$J_2^{(2)}\dot{\omega}_2^{(2)}(t) = s_{B3}P(t)$	$J_2^{(2)}\dot{\omega}_2^{(2)}(t) = s_{B3}\hat{R}(t)$
Body 2; *Rotation about 3*	$J_3^{(2)}\dot{\omega}_3^{(2)}(t) = -s_{B2}P(t)$	$J_3^{(2)}\dot{\omega}_3^{(2)}(t) = -s_{B2}\hat{R}(t)$

$$(27a, b, c, d)$$

We integrate all eight between their respective temporal boundaries, while reformulating the previous table using the Coefficient of Restitution, and parenthesize expressions for clarity.

TABLE 7
Integration of components of Euler's equation for each body during both phases

	Loading	Unloading
Body 1 Rot 2	$J_2^{(1)}\omega_2^{(1)}(t') - J_2^{(1)}\omega_2^{(1)}(t_1) = \left(-s_{A3}\int_{t_1}^{t'}P(t)\right)$	$J_2^{(1)}\omega_2^{(1)}(t_2) - J_2^{(1)}\omega_2^{(1)}(t') = e\left(-s_{A3}\int_{t_1}^{t'}P(t)\right)$
Body 1 Rot 3	$J_3^{(1)}\omega_3^{(1)}(t') - J_3^{(1)}\omega_3^{(1)}(t_1) = \left(s_{A2}\int_{t_1}^{t'}P(t)\right)$	$J_3^{(1)}\omega_3^{(1)}(t_2) - J_3^{(1)}\omega_3^{(1)}(t') = e\left(s_{A2}\int_{t_1}^{t'}P(t)\right)$
Body 2 Rot 2	$J_2^{(2)}\omega_2^{(2)}(t') - J_2^{(2)}\omega_2^{(2)}(t_1) = \left(s_{B3}\int_{t_1}^{t'}P(t)\right)$	$J_2^{(2)}\omega_2^{(2)}(t_2) - J_2^{(2)}\omega_2^{(2)}(t') = e\left(s_{B3}\int_{t_1}^{t'}P(t)\right)$
Body 2 Rot 3	$J_3^{(2)}\omega_3^{(2)}(t') - J_3^{(2)}\omega_3^{(2)}(t_1) = \left(-s_{B2}\int_{t_1}^{t'}P(t)\right)$	$J_3^{(2)}\omega_3^{(2)}(t_2) - J_3^{(2)}\omega_3^{(2)}(t') = e\left(-s_{B2}\int_{t_1}^{t'}P(t)\right)$

$$(28a, b, c, d)$$

We can now algebraically equate the left and right sides of each row, above.

$$e\,J_2^{(1)}\omega_2^{(1)}(t') - J_2^{(1)}\omega_2^{(1)}(t_1) = J_2^{(1)}\omega_2^{(1)}(t_2) - J_2^{(1)}\omega_2^{(1)}(t') \quad (29a)$$

$$e\,J_3^{(1)}\omega_3^{(1)}(t') - J_3^{(1)}\omega_3^{(1)}(t_1) = J_3^{(1)}\omega_3^{(1)}(t_2) - J_3^{(1)}\omega_3^{(1)}(t') \quad (29b)$$

$$e\,J_2^{(2)}\omega_2^{(2)}(t') - J_2^{(2)}\omega_2^{(2)}(t_1) = J_2^{(2)}\omega_2^{(2)}(t_2) - J_2^{(2)}\omega_2^{(2)}(t') \quad (29c)$$

$$e\,J_3^{(2)}\omega_3^{(2)}(t') - J_3^{(2)}\omega_3^{(2)}(t_1) = J_3^{(2)}\omega_3^{(2)}(t_2) - J_3^{(2)}\omega_3^{(2)}(t') \quad (29d)$$

Reformulate equations (29), (16) and (17) to obtain the critical values at the time of impact.

TABLE 8
The six unknown variables at the time of peak impact

ID at time t'	Expression
Body 1, Rotation about 2	$\omega_2^{(1)}(t') = \left(\omega_2^{(1)}(t_2) + e\omega_2^{(1)}(t_1)\right)/(1+e)$
Body 1, Rotation about 3	$\omega_3^{(1)}(t') = \left(\omega_3^{(1)}(t_2) + e\omega_3^{(1)}(t_1)\right)/(1+e)$
Body 2, Rotation about 2	$\omega_2^{(2)}(t') = \left(\omega_2^{(2)}(t_2) + e\omega_2^{(2)}(t_1)\right)/(1+e)$
Body 2, Rotation about 3	$\omega_3^{(2)}(t') = \left(\omega_3^{(2)}(t_2) + e\omega_3^{(2)}(t_1)\right)/(1+e)$
Body 1, Velocity of CM For the 1-direction	$v_{C1}^{(1)}(t') = \left(v_{C1}^{(1)}(t_2) + ev_{C1}^{(1)}(t_1)\right)/(1+e)$
Body 2, Velocity of CM For the 1-direction	$v_{C1}^{(2)}(t') = \left(v_{C1}^{(2)}(t_2) + ev_{C1}^{(2)}(t_1)\right)/(1+e)$

$$(30a, b, c, d, e, f)$$

We save these equations. We use them indirectly, as follows. We must eventually transfer the velocity expressions (last two rows, above) from the center of mass, to an equation concerning the contact point. For it is only then that we can apply the assumption that at peak time, the velocities of the two contact points are the same. The MFM gives us this power.

Thus, we digress one last time. We may assert, focusing on body 1 and point A, that the velocity of point A, is the velocity of the Center of Mass, plus the velocity of A as observed from moving point, C:

$$\mathbf{r}_A^{(1)} = \mathbf{r}_C^{(1)} + \mathbf{s}_{A/C}^{(1)} \quad (31a)$$

$$\mathbf{v}_A^{(1)} = \mathbf{v}_C^{(1)} + d\left(\mathbf{e}^{(1)}s_A^{(1)}\right)/dt \quad (31b)$$

$$\mathbf{v}_A^{(1)} = \mathbf{v}_C^{(1)} + \mathbf{e}^{(1)}\overrightarrow{\omega^{(1)}(t)}s_A^{(1)} = \mathbf{v}_C^{(1)} + \mathbf{e}^I R^{(1)}(t)\overrightarrow{\omega^{(1)}(t)}s_A^{(1)} \quad (31c)$$

Expending the terms, we find:

$$\mathbf{v}_A^{(1)}(t) = \mathbf{e}^I\left(\begin{Bmatrix} v_{C1}^{(1)}(t) \\ v_{C2}^{(1)}(t) \\ v_{C3}^{(1)}(t) \end{Bmatrix} + R^{(1)}\begin{Bmatrix} -s_{A2}^{(1)}\omega_3(t) + s_{A3}^{(1)}\omega_2(t) \\ s_{A1}^{(1)}\omega_3(t) - s_{A3}^{(1)}\omega_1(t) \\ -s_{A1}^{(1)}\omega_2(t) + s_{A2}^{(1)}\omega_1(t) \end{Bmatrix}\right) \quad (31d)$$

Similarly, we also find, for point B on Body 2:

$$\mathbf{v}_B^{(2)}(t) = \mathbf{e}^I\left(\begin{Bmatrix} v_{C1}^{(2)}(t) \\ v_{C2}^{(2)}(t) \\ v_{C3}^{(2)}(t) \end{Bmatrix} + R^{(2)}(t)\begin{Bmatrix} -s_{B2}^{(2)}\omega_3^{(2)}(t) + s_{B3}^{(2)}\omega_2^{(2)}(t) \\ s_{B1}^{(2)}\omega_3^{(2)}(t) - s_{B3}^{(2)}\omega_1^{(2)}(t) \\ -s_{B1}^{(2)}\omega_2^{(2)}(t) + s_{B2}^{(2)}\omega_1^{(2)}(t) \end{Bmatrix}\right) \quad (31e)$$

We assume there is no rotation during this finitely-small time of contact, meaning that the rotation matrix becomes the identity matrix $R^{(1)}(t') = R^{(2)}(t') = I_{3x3}$ Thus, this gives us the equations for the velocities at point A and B for body 1 and 2 to be:

$$\mathbf{v}_A^{(1)}(t) = \mathbf{e}^I \begin{pmatrix} v_{C1}^{(1)}(t) - s_{A2}^{(1)}\omega_3^{(1)}(t) + s_{A3}^{(1)}\omega_2^{(1)}(t) \\ v_{C2}^{(1)}(t) + s_{A1}^{(1)}\omega_3^{(1)}(t) - s_{A3}^{(1)}\omega_1^{(1)}(t) \\ v_{C3}^{(1)}(t) - s_{A1}^{(1)}\omega_2^{(1)}(t) + s_{A2}^{(1)}\omega_1^{(1)}(t) \end{pmatrix} \qquad (32a)$$

$$\mathbf{v}_B^{(2)}(t) = \mathbf{e}^I \begin{pmatrix} v_{C1}^{(2)}(t) - s_{B2}^{(2)}\omega_3^{(2)}(t) + s_{B3}^{(2)}\omega_2^{(2)}(t) \\ v_{C2}^{(2)}(t) + s_{B1}^{(2)}\omega_3^{(2)}(t) - s_{B3}^{(2)}\omega_1^{(2)}(t) \\ v_{C3}^{(2)}(t) - s_{B1}^{(2)}\omega_2^{(2)}(t) + s_{B2}^{(2)}\omega_1^{(2)}(t) \end{pmatrix} \qquad (32b)$$

We now impose our last and most critical restriction. We assume that at the peak moment of collision $t = t'$, the normal velocity of points A and B are the same. We apply this only for the 1-direction.

$$v_A^{(1)}(t') = v_B^{(2)}(t') \qquad (33)$$

$$v_{C1}^{(1)}(t') - s_{A2}^{(1)}\omega_3^{(1)}(t') + s_{A3}^{(1)}\omega_2^{(1)}(t') = v_{C1}^{(2)}(t') - s_{B2}^{(2)}\omega_3^{(2)}(t') + s_{B3}^{(2)}\omega_2^{(2)}(t') \quad (34)$$

Bookkeeping
In general, for any spatial contact, there are 12 unknowns: 3 final angular velocities and 3 final translational velocities; each, for two bodies.

The line of contact pre-determines the 1-axis. We have already asserted that contact is smooth in the 2 and 3 directions. This latter means no change in velocities along the tangent plane. We have also asserted that the contact will not affect the rotation about the collision axis: this means there is no change in the angular velocities about this axis. Thus, we have six unknowns, which we list here:

$$v_{C1}^{(1)}(t_2) \quad v_{C1}^{(2)}(t_2) \quad \omega_2^{(1)}(t_2) \quad \omega_2^{(2)}(t_2) \quad \omega_3^{(1)}(t_2) \quad \omega_3^{(2)}(t_2)$$

We have established two equations already:

- Identical material contact point velocity (34)
- Conservation of linear momentum in 1-direction (13)

We need four more equations. We obtain these *adding* the left and right column of each row of Table 7 to obtain a kinetic expression for the duration of impact. We do the first row:

$$J_2^{(1)}\omega_2^{(1)}(t') - J_2^{(1)}\omega_2^{(1)}(t_1) + J_2^{(1)}\omega_2^{(1)}(t_2) - J_2^{(1)}\omega_2^{(1)}(t')$$
$$= \left(-s_{A3}\int_{t_1}^{t'} P(t) \right) + e\left(-s_{A3}\int_{t_1}^{t'} P(t) \right) \qquad (35)$$

$$-J_2^{(1)}\omega_2^{(1)}(t_1) + J_2^{(1)}\omega_2^{(1)}(t_2) = -s_{A3}\left(1+e\right)\int_{t_1}^{t'} P(t) \qquad (36)$$

To remove the term on the right above, we add (11a) and (12a) to obtain:

$$m^{(1)}\left(v_{C1}^{(1)}(t_1) - v_{C1}^{(1)}(t_2) \right) = (1+e)\int_{t_1}^{t'} P(t) \qquad (37)$$

We combine (37) and (36) and obtain, for that row and the other three, the final four equations, each recast with the unknowns on the left.

Row 1: $\quad J_2^{(1)}\omega_2^{(1)}(t_2) - s_{A3}m^{(1)}v_{C1}^{(1)}(t_2) = -s_{A3}m^{(1)}v_{C1}^{(1)}(t_1) + J_2^{(1)}\omega_2^{(1)}(t_1) \quad (38)$

Row 2: $\quad J_3^{(1)}\omega_3^{(1)}(t_2) + s_{A2}m^{(1)}v_{C1}^{(1)}(t_2) = s_{A2}m^{(1)}v_{C1}^{(1)}(t_1) + J_3^{(1)}\omega_3^{(1)}(t_1) \quad (39)$

Row 3: $\quad J_2^{(2)}\omega_2^{(2)}(t_2) + s_{B3}m^{(1)}v_{C1}^{(1)}(t_2) = s_{B3}m^{(1)}v_{C1}^{(1)}(t_1) + J_2^{(2)}\omega_2^{(2)}(t_1) \quad (40)$

Row 4: $\quad J_3^{(2)}\omega_3^{(2)}(t_2) - s_{B2}m^{(1)(1)}v_{C1}^{(1)}(t_2) = -s_{B2}m^{(1)}v_{C1}^{(1)}(t_1) + J_3^{(2)}\omega_3^{(2)}(t_1) \quad (41)$

NUMERICAL VALIDATION

For the case under study, we present the collision of two cuboids. We classify this as an eccentric impact, since the center of mass of the bodies are not on the line of collision. In this analysis, the blue cuboid, (cuboid (1)), is assigned a mass $m^{(1)} = 1000\,Kg$. Geometric values are:

$w^{(1)} = 4 \qquad h^{(1)} = 5 \qquad d^{(1)} = 2$
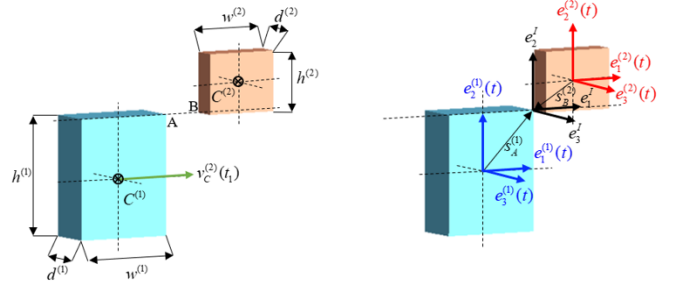$w^{(2)} = 3 \qquad h^{(2)} = 2.5 \qquad d^{(2)} = 1$

FIGURE 3. COLLISION OF TWO CUBOIDS

In this study, the blue cuboid is moving toward the orange cuboid with a velocity of 1 m/s. The orange cuboid is initially motionless. No object has an angular velocity prior to the collision. With this, we commence the analysis, leveraging the previous foundational work.

Using the previous frames, we first locate the point of contact.

The point of contact for cuboid (1) is predetermined to be:

$$\mathbf{s}_A^{(1)} = \mathbf{e}^{(1)}(t)\begin{pmatrix} s_{A1}^{(1)} \\ s_{A2}^{(1)} \\ s_{A3}^{(1)} \end{pmatrix} = \mathbf{e}^{(1)}(t)\begin{pmatrix} 2 \\ 2.5 \\ 1 \end{pmatrix} \qquad (a)$$

The point of contact for cuboid (2) is predetermined to be:

11

$$\mathbf{s}_B^{(2)} = \mathbf{e}^{(2)}(t)\begin{pmatrix} s_{B1}^{(2)} \\ s_{B2}^{(2)} \\ s_{B3}^{(2)} \end{pmatrix} = \mathbf{e}^{(2)}(t)\begin{pmatrix} -1.5 \\ -1.25 \\ -0.5 \end{pmatrix} \qquad (b)$$

Let us first reassert our six equations:

$$m^{(1)}v_{C1}^{(1)}(t_2) + m^{(2)}v_{C1}^{(2)}(t_2) = m^{(1)}v_{C1}^{(1)}(t_1) + m^{(2)}v_{C1}^{(2)}(t_1) \qquad (13)$$

$$v_{C1}^{(1)}(t') - s_{A2}^{(1)}\omega_3^{(1)}(t') + s_{A3}^{(1)}\omega_2^{(1)}(t') = v_{C1}^{(2)}(t') - s_{B2}^{(2)}\omega_3^{(2)}(t') + s_{B3}^{(2)}\omega_2^{(2)}(t') \quad (34)$$

$$J_2^{(1)}\omega_2^{(1)}(t_2) - s_{A3}m^{(1)}v_{C1}^{(1)}(t_2) = -s_{A3}m^{(1)}v_{C1}^{(1)}(t_1) + J_2^{(1)}\omega_2^{(1)}(t_1) \qquad (38)$$

$$J_3^{(1)}\omega_3^{(1)}(t_2) + s_{A2}m^{(1)}v_{C1}^{(1)}(t_2) = s_{A2}m^{(1)}v_{C1}^{(1)}(t_1) + J_3^{(1)}\omega_3^{(1)}(t_1) \qquad (39)$$

$$J_2^{(2)}\omega_2^{(2)}(t_2) + s_{B3}m^{(1)}v_{C1}^{(1)}(t_2) = s_{B3}m^{(1)}v_{C1}^{(1)}(t_1) + J_2^{(2)}\omega_2^{(2)}(t_1) \qquad (40)$$

$$J_3^{(2)}\omega_3^{(2)}(t_2) - s_{B2}m^{(1)(1)}{}_{C1}(t_2) = -s_{B2}m^{(1)}v_{C1}^{(1)}(t_1) + J_3^{(2)}\omega_3^{(2)}(t_1) \qquad (41)$$

We note that Eqn. (34) can be reformulated with the equations from Table 8. However, before doing that, we first simplify our equations for the case under study by asserting the following kinematic information prior to impact.

$$\omega_2^{(1)}(t_1) = \omega_3^{(1)}(t_1) = \omega_2^{(2)}(t_1) = \omega_3^{(2)}(t_1) = v_{C1}^{(2)}(t_1) = 0$$

After modifying Table 8, for the above zero-terms, we find:

$$m^{(1)}v_{C1}^{(1)}(t_2) + m^{(2)}v_{C1}^{(2)}(t_2) = m^{(1)}v_{C1}^{(1)}(t_1) \qquad (13)$$

$$\begin{aligned} v_{C1}^{(1)}(t_2) - v_{C1}^{(2)}(t_2) - s_{A2}^{(1)}\omega_3^{(1)}(t_2) + s_{A3}^{(1)}\omega_2^{(1)}(t_2) + \\ s_{B2}^{(2)}\omega_3^{(2)}(t_2) - s_{B3}^{(2)}\omega_2^{(2)}(t_2) = -ev_{C1}^{(1)}(t_1) \end{aligned} \qquad (34)$$

$$J_2^{(1)}\omega_2^{(1)}(t_2) - s_{A3}m^{(1)}v_{C1}^{(1)}(t_2) = -s_{A3}m^{(1)}v_{C1}^{(1)}(t_1) \qquad (38)$$

$$J_3^{(1)}\omega_3^{(1)}(t_2) + s_{A2}m^{(1)}v_{C1}^{(1)}(t_2) = s_{A2}m^{(1)}v_{C1}^{(1)}(t_1) \qquad (39)$$

$$J_2^{(2)}\omega_2^{(2)}(t_2) + s_{B3}m^{(1)}v_{C1}^{(1)}(t_2) = s_{B3}m^{(1)}v_{C1}^{(1)}(t_1) \qquad (40)$$

$$J_3^{(2)}\omega_3^{(2)}(t_2) - s_{B2}m^{(1)(1)}{}_{C1}(t_2) = -s_{B2}m^{(1)}v_{C1}^{(1)}(t_1) \qquad (41)$$

We recast all of these in matrix form for solution:

$$\begin{bmatrix} m^{(1)} & m^{(2)} & 0 & 0 & 0 & 0 \\ 1 & -1 & 0 & 0 & 0 & 0 \\ -s_{A3}m^{(1)} & 0 & J_2^{(1)} & 0 & 0 & 0 \\ s_{A2}m^{(1)} & 0 & 0 & J_3^{(1)} & 0 & 0 \\ s_{B3}m^{(1)} & 0 & 0 & 0 & J_2^{(2)} & 0 \\ -s_{B2}m^{(1)} & 0 & 0 & 0 & 0 & J_3^{(2)} \end{bmatrix} \begin{pmatrix} v_{C1}^{(1)}(t_2) \\ v_{C1}^{(2)}(t_2) \\ \omega_2^{(1)}(t_2) \\ \omega_2^{(2)}(t_2) \\ \omega_3^{(1)}(t_2) \\ \omega_3^{(2)}(t_2) \end{pmatrix} = \begin{pmatrix} m^{(1)}v_{C1}^{(1)}(t_1) \\ -ev_{C1}^{(1)}(t_1) \\ -s_{A3}m^{(1)}v_{C1}^{(1)}(t_1) \\ s_{A2}m^{(1)}v_{C1}^{(1)}(t_1) \\ s_{B3}m^{(1)}v_{C1}^{(1)}(t_1) \\ -s_{B2}m^{(1)}v_{C1}^{(1)}(t_1) \end{pmatrix}$$

RESULTS

We now compare the predictions of the MFM and MSC ADAMS. In all our tests, the geometries of the two bodies is as stated in the previous section. In all cases, the impact velocity of the first body is 1 meter/sec. In all cases, the mass of the first body—body (1)—is 1000 Kg. Thus, in all cases, the initial kinetic energy is 500 Joules.

We have not prohibited re-collision of the bodies (but this is straightforward to address).

We present tests wherein the bodies collide, face to face, edge to edge, and corner to corner. However, this restriction can easily be removed.

Before we proceed to the results, we discuss the visualization of the results of the MFM.

To provide a visualization of the calculations and to demonstrate how suitable MFM is for programming, we created a 3D simulation with Web Graphics Library (WebGL). WebGL is a JavaScript interface for rendering interactive 2D and 3D computer graphics. WebGL is compatible with most of the major web browsers such as Chrome, Firefox, Safari, and Opera. In addition, it is free and can be used without the need for plugins. Readers my view results on their own cell phones. The reader may confirm these results on this web page.

http://home.hib.no/prosjekter/dynamics/2019/contact/

Note also, that this web-based visualization, also reports the absolute kinematic results, whereas in the following discussion, we report the ratio of result between MFM and MSC.

In all cases—face-to-face, edge-to-edge, and corner-to-corner—the MFM and MSC agree on the final angular and linear velocities. In both cases, there is no increase in kinetic energy due to numerical integration effects. Linear momentum is of course, conserved.

Table 9 presents the results for Edge Collision. In this table, the coefficient of restitution changes, while the density ratio for the two bodies, remains as 1.0 (actual mass of the second body can be computed from this ratio, the mass of the first body and the volumes).

TABLE 9
Edge Collision with varying COR

			DENSITY RATIO = 1.00					
COR	$v_{C1}^{(1)}(t_2)$	$v_{C1}^{(2)}(t_2)$	$\omega_2^{(1)}(t_2)$	$\omega_2^{(2)}(t_2)$	$\omega_3^{(1)}(t_2)$	$\omega_3^{(2)}(t_2)$	ΔKE_{MFM}	ΔKE_{MSC}
1.00	1.0004	0.9984	1.0079	1.0158	0	0	0	1.400
0.75	0.9996	1.0016	0.9992	0.9983	0	0	25.650	25.600
0.50	0.9987	1.0062	1.0048	1.0032	0	0	43.950	44.300

Table 10 presents the results for Edge Collision. In this table, the density ratio varies from 0.5 to 1 and 2, for constant coefficient of restitution=0.75.

TABLE 10
Edge Collision with varying Density Ratio

	COEFFICIENT OF RESTITUTION = 0.75							
DR	$v_{C1}^{(1)}(t_2)$	$v_{C1}^{(2)}(t_2)$	$\omega_2^{(1)}(t_2)$	$\omega_2^{(2)}(t_2)$	$\omega_3^{(1)}(t_2)$	$\omega_3^{(2)}(t_2)$	ΔKE_{MFM}	ΔKE_{MSC}
0.50	0.9962	1.0074	0.9952	0.9884	0	0	43.175	42.400
1.00	0.9996	1.0016	0.9992	0.9983	0	0	25.650	25.600
2.00	1.0015	0.9893	0.9882	1.0525	0	0	14.150	14.410

Table 11 presents the results for Corner Collision. In this table, the coefficient of restitution changes, while the density ratio for the two bodies, remains as 1.0.

TABLE 11
**Corner Collision with varying COR**

	DENSITY RATIO = 1.00							
COR	$v_{C1}^{(1)}(t_2)$	$v_{C1}^{(2)}(t_2)$	$\omega_2^{(1)}(t_2)$	$\omega_2^{(2)}(t_2)$	$\omega_3^{(1)}(t_2)$	$\omega_3^{(2)}(t_2)$	ΔKE_{MFM}	ΔKE_{MSC}
1.00	1.0068	0.9514	0.9301	0.9221	0.9620	0.9668	0.050	-5.500
0.75	1.0033	0.9718	0.9559	0.9489	0.9783	0.9812	12.930	10.850
0.50	1.0009	0.9906	0.9794	0.9742	0.9957	0.9981	22.165	21.940

Table 12 presents the results for Corner Collision. In this table, the density ratio varies from 0.5 to 1 and 2, for constant coefficient of restitution=0.75.

TABLE 12
Corner Collision with varying Density Ratio

	COEFFICIENT OF RESTITUTION = 0.75							
DR	$v_{C1}^{(1)}(t_2)$	$v_{C1}^{(2)}(t_2)$	$\omega_2^{(1)}(t_2)$	$\omega_2^{(2)}(t_2)$	$\omega_3^{(1)}(t_2)$	$\omega_3^{(2)}(t_2)$	ΔKE_{MFM}	ΔKE_{MSC}
0.50	1.0109	0.9508	0.9451	0.9437	0.9520	0.9526	21.500	14.100
1.00	1.0033	0.9718	0.9559	0.9489	0.9783	0.9812	12.930	10.850
2.00	1.0013	0.9794	0.9355	0.9769	0.9918	0.9930	7.195	6.600

There will come a day when PDF research papers come with embedded WebGL windows. Until then, we provide, below, as a perfunctory gesture, two snapshots of post collision behavior. Naturally, these pale in comparison to the actual 3D web page listed above, which the reader should consult.
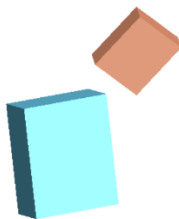
FIGURE 4. CORNER POST COLLISION

In Figure 4 we display the cuboids shortly after the collision taken from MSC ADAMS. The coefficient is set to 1.0 and the density ratio of the material of the cuboids are 1.0. Here we see both cuboids rotation about the 2- and 3-axis of their moving frames (all be it very slowly for Cuboid 1), which makes them rotate about every axis from an inertial point of view.

FIGURE 5. EDGE POST COLLISION

The collision in Figure 5 have the same set of values for the coefficient of restitution and density ratio as the collision of Figure 4. This is taken some time after the collision. Here we see the cuboids rotate about the 2-axis of their moving frames, and since there is only one rotation, it looks the same from inertial.

DISCUSSION

Various methods exist for collision analysis. Many involve incremental analyses that which ensures no body penetration. Often, these results require time stepping. This, in turn, allows for varied constitutive laws.

The MFM presents a structured, geometric approach to model collisions. We obtain the same results as in commercial software. However, we have noted that our results are algebraic in nature, require no time stepping and are rapid to obtain, and easily coded.

The results indicate that the MFM can structure a collision analysis and produce the same results as MSC, but faster—so fast, the analysis runs on a cell phone.
If desired, the analyst may readily insert friction in the tangential directions.

Another, modification, with greater potential, is to modify the rotation matrices and make them time dependent.
Furthermore, future work could assert that the moment arms to the collision points from the center of mass of each body, are also time dependent.

Any constitutive model may be inserted into this geometric structure.

In the future, one may supplement this approach with an algorithm to detect the points on incipient collision. From there, one defines the collision axis; then one constructs one more orthogonal axis and, finally, the third one in accordance with the right hand rule.

Finally, one may also then supplement this approach with a method to obtain moment of inertia matrices that are not necessarily diagonal. However, this is not a substantive challenge.

For now, however, we close this paper with the statement that the MFM presents a very inexpensive, extensible, and simple model of collisions.

REFERENCES

[1] Wu, C.-Y., Li, L.-Y., and Thornton, C., "Energy Dissipation During Normal Impact of Elastic and Elastic-Plastic Spheres." International Journal of Impact Engineering, 32(1-4), 593-604.

[2] Gilardi, G., and Sharf, I. "Literature Survey of Contact Dynamics Modeling." Mechanism and Machine Theory, 37(10), 1213-1239.

[3] Wang, Y., and Mason, J.T., "Two-Dimensional Rigid Body Collisions with Friction," Journal of Applied Mechancis, 59(3), 635.

[4] Minamoto, H., Seifried, R., Eberhard, P., and Kawamura, S. "Experimental and Numerical Analysis of Repeated Impacts between Two Spheres." Applied Mechanics and Materials, Vol. 566, pp. 250-255.

[5] Gharib, M. and Hurmuzlu, Y. "A New Contact Force Model for Low Coefficient of Restitution Impact." Journal of Applied Mechanics, 79 (6), 064506

[6] Hunt, K.H., and Crossley, F.R.E. "Coefficient of Restitution Interpreted as Damping in Vibroimpact." Journal of Applied Mechancis, 42(2), 440.

[7] Ahmad, J., Ismail, K.A., and Mat, F. "Impact Models and Coefficient of Restitution: A Review." APN Journal of Engineering and Applied Sciences, Vol. 212, No. 210, May 2016

[8] Cross, R., "Measurements of the horizontal coefficient of Restitution for a Superball and a Tennis Ball." American Journal of Physics, 70(5), 482

[9] Batista, M., "On the Mutual Coefficient of Restitution in Two Car Collinear Collisions," Retrieved from https://arxiv.org/abs/physics/0601168, DOA April, 24, 2019

[10] Vasilopolous, V., Paraskevas, I.S., and Papadopoulos, E. G.. "Compliant Terrain Legged Locomotion Using a Viscoelastic Approach, IROS 4849-4854.

[11] Cartan, É, 1986, On Manifolds with an Affine Connection and the Theory of General Relativity, translated by A. Magnon and A. Ashtekar, Napoli, Italy, Bibiliopolis.

[12] Frankel T, (2012) The Geometry of Physics, an Introduction, third edition, Cambridge University Press, New York; First edition published in 1997.

[13] Impelluso, T., 2017, "The moving frame method in dynamics: Reforming a curriculum and assessment," International Journal of Mechanical Engineering Education. https://doi.org/10.1177/0306419017730633
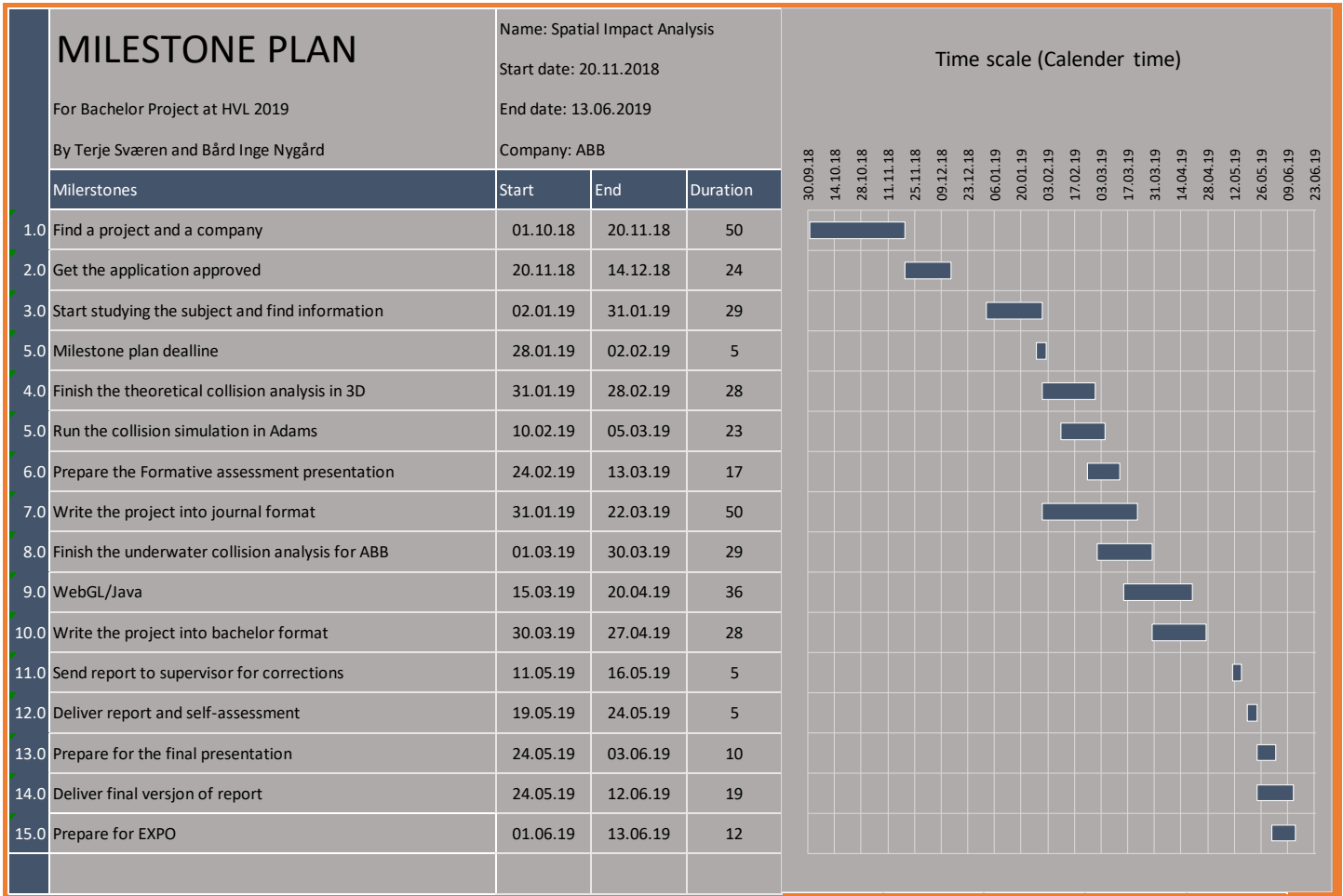
[14] https://www.khronos.org/webgl/

FLOW CHART

At the start of the semester, we made a flow chart/milestone plan (see next page) to get an overview of the task at hand. Throughout the semester we have been comparing our work with this chart and used it as an indicator of our progress.

To further specify what we had to do to complete our milestones, we also made a timetable with sub-objects that lead up to the main milestones.

TIMETABLE			Status:	Started and everything is OK
For Bachelor project at HVL 2019				Started but with minor problems
To do list:	Start date	End date	Status	Started but with serious problems / Finished
1.0 Find a project and a company	01.10.18	20.11.18		☑
1.1 Create a group				☑
1.2 Find a interesting project				☑
1.3 Get in touch with the supervisor				☑
1.4 Get in touch with the company				☑
2.0 Get the application approved	10.02.19	05.03.19		☑
2.1 Write and submit an abstract				☑
2.2 Set up a meeting with the company				☑
2.3 Get a supervisor from the company				☑
2.4 Set the bounderies of the project with the company				☑
2.5 Sign necessary contracts				☑
3.0 Start studying the subject and find information	02.01.19	31.01.19		☑
3.1 Read and understand chapter 9.3				☑
3.2 Convert chapter 9.3 from 2D to 3D				☑
3.3 Look through collision examples from textbooks that uses traditional dynamics				☑
3.4 Look through collision examples that uses the Moving Frame Method				☑
3.5 Learn how to simulate in MSC Adams				☑
4.0 Finish the theoretical collision analysis in 3D	28.01.19	02.02.19		☑
4.1 Make a general example of two bodies colliding in 3D				☑
4.2 Set some parametres (time of impact, etc)				☑
4.3 Calculate the coefficient of restitution				☑
4.3 Calculate the forces and projectiles				☑
5.0 Run the collision simulation in Adams	31.01.19	28.02.19		☑
5.1 Make models in Creo				☑
5.2 Convert the models to MSC Adams files				☑
5.3 Run simulations with the same parametres as in the theoretical analysis				☑
5.4 Compare results				☑
5.5 Make the simulation presentable to the company				☑
6.0 Prepare the Formative assessment presentation	10.02.19	05.03.19		☑
6.1 Make a powerpoint presentation				☑
6.2 Write a script and assign parts				☑
6.3 Rehearse				☑
7.0 Write the project into journal format	24.02.19	13.03.19		☑
7.1 Absctract				☑
7.2 Intro				☑
7.3 Background				☑
7.4 Main				☑
7.5 Conclusion				☑
8.0 Finish the underwater collision analysis for ABB	31.01.19	22.03.19	(red/yellow)	☐
8.1 Gather all the requiered information from ABB				☐
8.2 Calculate the forces from the impact			(red)	☐
8.3 Analyse the impact using MSC Adams			(red)	☐
8.4 Conclude			(red)	☐
9.0 WebGL/Java	01.03.19	30.03.19		☑
9.1 Learn WebGL and Java				☑
9.2 Gather pre-existing codes and write the necessary new ones				☑
9.3 Create a simple collision simulation				☑
10.0 Write the project into bachelor format	15.03.19	20.04.19		☑
10.1 Frontpage (Forside_bacheloroppgave.doc)				☑
10.2 Intro (Rapport_bacheloroppgave.doc)				☑
10.3 Abstract				☑
10.4 Method				☑
10.5 Results				☑
10.6 Discussion				☑
10.7 Conclusion				☑
10.8 Referance list				☑
10.9 Attachments				☑
10.10 Backside (Bakside_bacheloroppgave.doc)				☑
11.0 Send report to supervisor for corrections	30.03.19	27.04.19		☑
11.1 Check report before posting				☑
12.0 Deliver report and self-assessment	11.05.19	16.05.19		☑
12.1 Fix corrections in the report				☑
12.2 Write self-assessment				☑
13.0 Prepare for the final presentation	19.05.19	24.05.19	(yellow)	☐
13.1 Make a Powerpoint presentation				☐
13.2 Write script and assign parts				☐
13.3 Rehearse				☐
14.0 Deliver final versjon of report	24.05.19	03.06.19		☑
14.1 Make final adjustments				☑
14.2 Hope that everything is OK				☑
15.0 Prepare for EXPO	24.05.19	12.06.19	(yellow)	☐

MILESTONE PLAN

For Bachelor Project at HVL 2019

By Terje Sværen and Bård Inge Nygård

Name: Spatial Impact Analysis

Start date: 20.11.2018

End date: 13.06.2019

Company: ABB

Time scale (Calender time)

	Milerstones	Start	End	Duration
1.0	Find a project and a company	01.10.18	20.11.18	50
2.0	Get the application approved	20.11.18	14.12.18	24
3.0	Start studying the subject and find information	02.01.19	31.01.19	29
5.0	Milestone plan dealline	28.01.19	02.02.19	5
4.0	Finish the theoretical collision analysis in 3D	31.01.19	28.02.19	28
5.0	Run the collision simulation in Adams	10.02.19	05.03.19	23
6.0	Prepare the Formative assessment presentation	24.02.19	13.03.19	17
7.0	Write the project into journal format	31.01.19	22.03.19	50
8.0	Finish the underwater collision analysis for ABB	01.03.19	30.03.19	29
9.0	WebGL/Java	15.03.19	20.04.19	36
10.0	Write the project into bachelor format	30.03.19	27.04.19	28
11.0	Send report to supervisor for corrections	11.05.19	16.05.19	5
12.0	Deliver report and self-assessment	19.05.19	24.05.19	5
13.0	Prepare for the final presentation	24.05.19	03.06.19	10
14.0	Deliver final versjon of report	24.05.19	12.06.19	19
15.0	Prepare for EXPO	01.06.19	13.06.19	12

Looking back, we now see that we were quite off on a number of things. Most importantly, the theoretical collision analysis (4.0) took way longer than we had anticipated to finish. And as a result of that, we had to work on many of the later objectives (such as 5.0, 7.0 and 9.0) at the same time as we worked on the theoretical collision analysis.

This delay made us unable to look into the underwater collision analysis that we had talk about with ABB. We always knew that there was a chance that we had taken on too much with this project, and the cooperation with ABB was always set as an addition to our project, but it is still unfortunate that we didn't get the time to test our new collision model on their problem.

Still, the main object of our project was to develop a new model for impact analysis, and that we did.